

Empirical Modeling of Kinetics of Transesterification and Cold Flow Properties of Used Soya Oil Biodiesel

Umeuzuegbu J.C.

Department of Chemical Engineering, Faculty of Engineering,
Chukwuemeka Odumegwu Ojukwu University, Anambra State, Nigeria

ABSTRACT

This research work focused on empirical modeling of kinetics of transesterification and cold flow properties of homogeneous catalyzed used soya oil fatty acid methyl ester (USOFAME). Used soya oil (USO) was prepared by frying food (yam, potato plantain etc) with virgin soya oil for a total of 72 hours [1]. The oil was characterized based on American Society for Testing and Materials (ASTM) method. The fatty acid profile of used soya oil was analyzed using gas chromatography mass spectroscopy (GC MS) while the functional groups of the triglyceride were determined using Fourier transform infrared spectroscopy (FTIR). The oil was pretreated to reduce the free fatty acid level below 1% and then transesterified using methanol in the presence of sodium hydroxide catalyst. The fuel properties of the USOFAME produced were determined based on ASTM standards. Kinetic experiments were conducted in batches at different temperatures of 450C, 550C and 650C. Application of rate laws to the three-step reversible reaction scheme of transesterification yielded a series of ordinary differential equations (ODEs) solved with polymath 5.1 software to give the forward and reverse rate constants k_1, k_2, k_3, k_4, k_5 and k_6 from which the rate limiting step (RLS) and activation energy (ΔE) were derived. The cold flow properties, cloud point (CP), cold filter plugging point (CFPP) and pour point (PP) were determined experimentally for different blends of biodiesel with #2 diesel, at a percentage volume ratio of biodiesel to diesel 0, 20, 40, 60, 80, and 100. The values obtained for CP, CFPP, and PP were plotted against the biodiesel fraction in the blends. Least square regression of the data of the plots were tested on linear, quadratic and polynomial models using Microsoft excel. The fuel properties of the USOFAME which is within the ASTM standards were determined as acid value 0.4mgKOH/g, density 863mm²/s, kinematic viscosity 4.60mm²/s, flash point 1620C, cetane number 61.00, calorific value 40.06MJ/Kg, pour point -40C, cold filter plugging point -2.80C, cloud point 00C, iodine value 30.60gI₂/100g. Kinetic modeling of transesterification of USOFAME shows that the forward rate constants K_1, K_2 , and K_3 are greater than those of the reverse reaction k_2, k_4, k_6 , imply that the forward reaction dominates while the reverse reaction could be neglected. The rate constant k_1 for triglyceride conversion to diglyceride is the least among the forward rate constants at 450C, 550C and 650C imply that this step is the rate limiting step (RLS). Application of least square regression analysis of Microsoft excel on the data of variation of cold flow properties with biodiesel fraction, revealed polynomial model to be the best fitting equation.

Keywords

Characterization, cold flow properties, kinetic modeling, transesterification, used soya oil fatty acid methyl ester.

1. INTRODUCTION

The soaring demand for energy and industrial raw materials from crude oil has hastened the depletion of its reserves, coupled with the adverse environmental impact and the unstable international market has compelled researchers to look for alternative fuel and raw material sources to fill the gap. Oils and fat from plants and animals has proved alternative sources as they are readily converted to biodiesel by suitable methods. Among the various options investigated, for fossil oil replacement, biodiesel produced from vegetable oil and other sources has been universally recognized as the foremost contender for exhaust emission reduction [2]. Burning of fossil fuel results in environmental pollution from emission of green house gases, including sulphur oxides (SO_x), nitrogen oxides (NO_x), carbon monoxide (CO), hydrocarbon (HC), and methane [3]. Biodiesel is a mono-alkyl ester of long chain fatty acid that posses characteristics similar to diesel with additional advantages of high lubricity, high cetane number, being biodegradable and environmentally friendly [4]. The bulk of biodiesel presently produced worldwide come from edible oil feed stock. The researcher [5] has reported that 95% of renewable resources used for biodiesel production come from edible vegetable oil, and this has been envisaged to have serious implication on food availability and the cost of biodiesel. As a result, concerted effort has being geared towards the production of biodiesel from non-edible oils and used cooking oils (UCO) feed stock. Used cooking oils have many disposal problems like water and soil pollution, human health concern, and disturbance to aquatic ecosystem [6]. Rather than its disposal that is harmful to the environment, it can be used as cost-effective feedstock for production of biodiesel. Biodiesel is produced by the reaction of fat with monohydric alcohol. Various processes have been adopted for biodiesel production from vegetable oil and animal fat, namely; micro-emulsion with alcohol, catalytic cracking, pyrolysis and transesterification [7], [8], [9], [10]. Among these methods, transesterification is the key and the most important process for production of a cleaner and environmentally safe biodiesel [11], [12]. Worldwide, biodiesel production is mainly from edible oils such as soybean, sunflower canola, palm oil etc. Utilization of edible oils as feedstock for biodiesel production poses a lot of concerns as this practice competes with food supply leading to high cost of edible vegetable oil, and consequently results in relative increase in biodiesel production

cost. Therefore, concerted research efforts are geared towards evaluating non-edible oils and waste cooking oil (WCO) or used cooking oil (UCO) as suitable feedstock. Used cooking oil or used oil for short refers to used vegetable oil obtained from cooking or frying of food. Repeated frying for preparation of food make such an oil unsuitable for consumption due to high free fatty acid content [12]. In order to minimize the market prize of edible oil and stem the contentious debate on the ill effect of use of edible oil for biodiesel production, research is now geared towards the use of UCO feedstock [13], [14], [15]. In order to carry out the research on a particular used oil (soya oil), used soya oil was prepared by frying foods (yam, potato plantain etc) in a virgin soya oil for a total of 72 hours [1]. The resulting used soya oil was then synthesized into biodiesel of which the kinetics of transesterification and cold flow temperature operability were modeled. The kinetics of transesterification of biodiesel has in the past been based on the stoichiometry of the reaction which assumed a single reaction step. However transesterification involves a series of reaction steps for conversion of triglyceride to biodiesel. The research work on kinetics focused on modeling the kinetics of homogeneous catalyzed transesterification of used soya oil based on appropriate reaction mechanism of multiple steps and empirical results of kinetic experiments. Researchers [16] and [17] have predicted cold flow properties of biodiesel based on the total unsaturated fatty acid methyl ester and on the biodiesel fraction in the blend. As the amount of unsaturated fatty acid and their chain length in the biodiesel is directly related to the biodiesel fraction in the blend, the cold flow properties of the biodiesel blend can be correlated with biodiesel fraction. The research work on cold flow properties is focused on modeling of the temperature operability of the USOFAME based on the biodiesel fraction in the blend.

2. MATERIALS AND METHODS

2.1 Materials

Used soya oil, reagents, glass wares, equipments including gas chromatography mass spectrometer (GC-MS), Fourier transform infrared spectroscopy (FTIR), viscometer, magnetic hot plate, water bath, polymath 5.1 software etc.

2.1.1 Preparation of used soya oil

10 liters out of 20 liters of crude soy oil purchased from Ogbote main market Enugu, in Enugu state was introduced into 20 liter steel pot. The oil was heated using gas cooker for frying foods (yam, plantain and potatoes) for a duration of 72hours (8 hours per day for 9 days) and then cooled to make waste or used cooking oil [1]. A test of the acid values showed much increase in the acid value from 0.23mg/g for the pure oil to 4.60mg/g for the used oil.

2.1.2 Characterization of used soya oil

The physiochemical properties of the used soya oil was characterized based on American Society for Testing Materials, ASTM 6751 (1973) method. Analytical equipments, GC- MS (QP2010 plus Shimadzu, Japan) and FTIR (M530 Bulk scientific FTIR) were used to determine the fatty acid profile and the functional groups of the oil respectively.

2.1.3 Pretreatment of the used soya oil

As the free fatty acid of the used soya oil exceeded the tolerable limit of 1% for transesterification of oil using alkaline catalyst, the oil was first of all pretreated with methanol in the presence of sulphuric acid to reduce the free fatty acid below 1%. The

pretreatment or esterification of the oil involve heating the oil on a heating mantle to 1100C for 10 minutes to drive off available moisture in the oil. This was followed by cooling the oil to 600C in a water bath. The oil was then introduced into a 500ml round bottomed flask and then the mixture of methanol of 60% w/w of oil and sulphuric acid 7% w/w of oil was added. Into the middle arm of the flask was fitted a reflux condenser, and a thermometer into the sample through the side arm. The setup was heated using a magnetic heating mantle to a constant temperature of 600C for 1 hour at an agitation speed of 350rpm. when the heated and refluxed content of the flask was transferred into 250ml separating funnels. After settling, the funnel content separates into three layers, water at the bottom, pretreated oil in the middle and methanol at the upper layer. The three layers were carefully tapped off separately, water first, followed by the oil and finally methanol. Hot distilled water was poured into the oil in a separating funnel, shaken and allowed to stand when it separated into water and oil layers below and above the funnel respectively. The water layer was tapped off from the separating funnel and the pre-treated oil was poured into 250ml beakers and dried carefully in an oven regulated at a temperature of 1050C until the residual water evaporated completely. After this process, the pre-treated oil was made ready for transesterification [18].

2.1.4 USOFAME Production and purification

The esterified oil was transesterified using methanol and sodium hydroxide catalyst. A 500ml three-necked round bottomed flask fitted with a condenser on the middle arm, a thermometer and sample outlet on the side arms respectively served as the reactor. The heating system consists of an electromagnetic hot plate which heats the reactor and rotates the metal knob in the reactor through an electromagnetic field. Specified quantity of the oil sample was introduced into the flask and the flask content heated to the temperature established for the reaction. Then methanol and the catalyst sodium hydroxide (NaOH) mixture was added in the amount established for the reaction, and the stirrer switched on at a specified speed, taking this moment as zero time of the reaction. The reaction mixture was vigorously stirred and refluxed for the required reaction time. At the end of methanolysis, the transesterified product was made to stand for a day in separating funnels where it separates into the upper biodiesel layer and the lower glycerol layer. The lower glycerol layer was tapped off first followed by the upper biodiesel layer. After transesterification, the upper ester layer may contain traces of methanol and glycerol. The remaining un-reacted methanol has safety risk and might corrode engine components, and glycerin within the biodiesel may lessen the fuel lubricity and cause injector coking and other deposits [19]. Such trace of methanol is soluble in water and is therefore removed by wet washing. The methyl ester or biodiesel layer was gently washed with hot distilled water in the ratio of 3:1 water to methyl ester. The methyl ester was gently washed to prevent its loss due to formation of emulsion that results in complete phase separation [20]. The washed biodiesel was dried by heating at 1050C on a laboratory hot plate until all residual water molecules is evaporated. This conforms with the findings of [21]. The percentage biodiesel yield is given by the expression of equation (1)

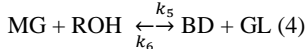
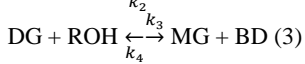
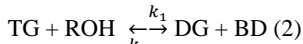
$$\% \text{ biodiesel yield} = \frac{\text{Volume of biodiesel produced}}{\text{volume of oil used}} \times 100 \quad (1)$$

2.2 Determination of fuel properties of USOFAME

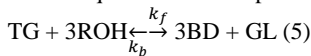
The properties of the biodiesel fuel were characterized based on ASTM standards. The properties characterized include density, viscosity, iodine value, saponification value, cetane number, acid value, free fatty acid, calorific value, flash point, cloud point, pour point and cold filter plugging point.

2.3 Kinetics of transesterification of USO

The kinetics of homogeneous transesterification of used soya oil using methanol and NaOH catalyst was studied. This involved kinetic modeling and kinetic experiment on transesterification of used soya oil. Transesterification of triglyceride (TG) consist of series of reversible reaction steps involving conversion of triglyceride to diglyceride (DG), diglyceride to monoglyceride (MG) and monoglyceride to biodiesel (BD) and a byproduct glycerol (GL) using methanol (MN) and NaOH catalyst as shown in equations 2 to 4. However, the kinetics of such reactions is first order with respect to the reacting component's concentration as shown in equations 2 to 4 [1]. Applying the rate law to equations 2 to 4 yielded a system of ordinary differential equations (ODE's) 6 to 25. Kinetic experiments were carried out in batches at different temperatures of 450C, 550C and 650C. Samples were withdrawn from the reaction mixture of the kinetic experiments at 15 minutes interval from 0 to 90 minutes and the concentration of the TG, DG, MG, BD, MN, and GL of the samples were determined using GC-MS. The concentration of the TG, DG, MG, BD, MN and GL denoted by [TG], [DG], [MG], [BD], [MN] and [GL] respectively were inserted into the ODE's and then solved using polymath 5.1 software to obtain the rate constants k1 to k6 at different temperatures of 450C, 550C and 650C.



where k_1, k_3 and k_5 are the forward rate constants while k_2, k_4 and k_6 are the reverse rate constants. Each of the three steps consumes 1 mole of alcohol to produces 1 mole of ester and the overall equation can be represented by equation (5) below.



where, k_f = rate constant for forward reaction, k_b = rate constant for backward reaction

Equations (2) to (4) yielded 6 elementary reactions, unto which the application of rate law generate a system of ordinary differential equations (6) to (25). The solution of equations (6), (10), (14), (19), (20) and (25) using polymath 5.1 gave the values of the rate constants k1 to k6

$$r_{TG} = -\frac{d[TG]}{dt} = k_1[TG][ROH] - k_2[DG][BD] \quad (6)$$

Similarly, other rate expressions were also derived in the same manner as follows:

$$r_{DG} = r_{DG1} + r_{DG2} \quad (7)$$

$$r_{DG1} = -\frac{d[DG]}{dt} = k_2[DG][BD] - k_1[TG][ROH] \quad (8)$$

$$r_{DG2} = -\frac{d[DG]}{dt} = k_3[DG][ROH] - k_4[MG][BD] \quad (9)$$

$$r_{DG} = k_3[DG][ROH] - k_1[TG][ROH] + k_2[DG][BD] - k_4[MG][BD] \quad (10)$$

$$r_{MG} = r_{MG1} + r_{MG2} \quad (11)$$

$$r_{MG1} = k_4[MG][BD] - k_3[DG][ROH] \quad (12)$$

$$r_{MG2} = k_5[MG][ROH] - k_6[BD][GL] \quad (13)$$

$$r_{MG} = k_5[MG][ROH] - k_6[BD][GL] + k_4[MG][BD] - k_3[DG][ROH] \quad (14)$$

$$r_{BD} = r_{BD1} + r_{BD2} + r_{BD3} \quad (15)$$

$$r_{BD1} = k_2[DG][BD] - k_1[TG][ROH] \quad (16)$$

$$r_{BD2} = k_4[MG][BD] - k_3[DG][ROH] \quad (17)$$

$$r_{BD3} = k_6[BD][GL] - k_5[MG][ROH] \quad (18)$$

$$r_{BD} = k_2[DG][BD] - k_1[TG][ROH] + k_4[MG][BD] - k_3[DG][ROH] + k_6[BD][GL] - k_5[MG][ROH] \quad (19)$$

$$r_{GL} = -k_5[MG][ROH] + k_6[BD][GL] \quad (20)$$

$$r_{ROH} = r_{ROH1} + r_{ROH2} + r_{ROH3} \quad (21)$$

$$r_{ROH1} = k_1[ROH][TG] - k_2[DG][BD] \quad (22)$$

$$r_{ROH2} = k_3[ROH][DG] - k_4[MG][BD] \quad (23)$$

$$r_{ROH3} = k_5[ROH][MG] - k_6[G][BD] \quad (24)$$

$$r_{ROH} = k_1[ROH][TG] - k_2[DG][BD] + k_3[ROH][DG] - k_4[MG][BD] + k_5[ROH][MG] - k_6[G][BD] \quad (25)$$

$$K = Ae^{-E/RT} \quad (26)$$

$$\ln k = \ln A - E/RT \quad (27)$$

Temperature dependency of rate constant

The dependency of rate constant on temperature is well represented by Arrhenius equation (26). Taking the log of equation (26) gave equation (27). From equation (27) the plot of $\ln k$ versus $1/T$ gave the slope $-E/R$ from which the activation energy (E) was obtained. where A is the frequency factor, R is the universal gas constant (Jmol⁻¹K⁻¹) and E is the activation energy (Jmol⁻¹). The plots of $\ln k$ versus $1/T$ are given in figures 3 to 8, and the values of the activation energy are given in table 4.

2.4 Modeling the effect of biodiesel blending on cold flow properties

Researchers [16], and [17] have correlated cold flow properties of biodiesel as a function of total unsaturated fatty acid methyl ester and as a function of biodiesel fraction in the blend respectively. Since the degree of un-saturation of fatty acid methyl ester is directly related to the biodiesel fraction in the blend, the cold flow properties, cloud point (CP), pour point (PP) and cold filter plugging point (CFPP) in this work were predicted based on the biodiesel fraction in the blend. Polynomial model has been employed in the past for prediction of cold flow properties as a function of biodiesel fraction. Here, apart from polynomial model, other predicting model equations including linear and exponential models were evaluated in order to obtain the best equation of fit. The fitting equations are:

$$Y = a + bx \quad (1)$$

$$Y = cedx \quad (2)$$

$$Y = f + gx + hx^2 \quad (3)$$

where Y's are the dependent variable or response (CP, CFPP, PP) and x the independent variable (biodiesel fraction in the blends). a, b, c, d, f, g and h are model correlation coefficients.

2.5 Blending of the used soya oil biodiesel with petro-diesel.

The used soya oil biodiesel was blended with #2 diesel oil on a percentage volume ratio of biodiesel to diesel ; 0, 20, 40, 60, 80 and 100 designated as B0, B20, B40, B60, B80 and B100 respectively. Direct blending of the required volumes of the biodiesel and diesel was carried out in conical flasks with continuous stirring to achieve uniformity of mixing.

3 RESULTS AND DISCUSSION

3.1 Characteristics of Used Soya Oil

The summary of the characteristics of used soya oil are presented in the Table1, From the table, it is seen that the free fatty of the used soya oil (2.10%) is greater than 1%, and therefore need be reduced below 1% for effective transesterification with alkali catalyst. Alkali catalysis of oils of high free fatty acid has high tendency for soap formation, reduction in biodiesel formation as a result of inhibition of the separation of esters from glycerol [22]. This accounts for pretreatment of the oil before esterification with alkali catalyst.. The kinematic viscosity measures the flow resistance of the fuel while the density of the oil plays a role in its measurement since this is determined volumetrically. The kinematic viscosity and the density of the oil ($47.78\text{mm}^2\text{s}^{-1}$ and 962kg/m^3) are higher than those of the biodiesel produced from it ($4.60\text{mm}^2\text{s}^{-1}$ and 863kg/m^3) and even much higher than that of diesel ($4.2\text{mm}^2\text{s}^{-1}$ and 835kg/m^3). High density and viscosity make atomization of the oil in internal combustion engine difficult and has been associated with increase in engine deposits, hence they cannot be used directly as bio-fuel [23]. The determined density of the oil 962kg/m^3 is in agreement with the literature findings of [20] but at variance with [24] and [25].

Iodine value, a measure of degree of un-saturation of the oil was obtained for USO as $75.4\text{gI}_2/\text{g}$ is below $100\text{gI}_2/100\text{g}$ oil, indicative of the oil being nondrying and therefore suitable for biodiesel production. High iodine value of oil corresponds to high degree of un-saturation of the fatty acid in the triglyceride. If heated, such oil is prone to thermal oxidation and polymerization of the triglyceride causing formation of deposits. The calorific value of used soya oil like that of any oil is relatively lower than that of diesel. The cloud and pour point of 5°C and -0.5°C respectively determined for the used soya oil are relatively low but not to the extent of being suitable for operation and handling during cold weather especially in cold climates. Peroxide value, an index of rancidity obtained as 9.5meq/kg was high and indicative of poor resistance of the oil to peroxidation during heating, storage and handling. The saponification value determined as 198.5 is in agreement with literature findings of [26] and [27].

Table 1: Physiochemical properties of USO oil

Properties	Unit	USO
Acid value	mgKOH/g	4.20
Free fatty acid	%	2.10
Saponification value	mgKOH/g	187.5
Iodine value	($\text{gI}_2/100\text{g}$ oil)	75.4
Peroxide value	meq/kg	9.5
Kinematic viscosity	mm^2s^{-1} @ 400C	47.78
Fire point	0C	280
Flash point	0C	180
Cloud point	0C	5
Pour point	0C	-5
Refractive index		0.4112
Specific gravity		0.962
Moisture content	%	0.2
Density	Kg/m^3	962
Calorific value	MJ/kg	34.20

3.2 The Fatty Acid Profile of Used Soya Oil

The fatty acid profile of used soya oil was determined using gas chromatography mass spectrometry (GC-MS). Figure1 shows the GC-MS spectra of used soya oil. The summary of fatty acid composition of used soya oil is shown in Table 2. Used soya oil consist of 32.64% of saturated acids (myristic acid, stearic acid, palmitic acid and arachidic acid) and 53.67% unsaturated acids (oleic acid, linoleic acid , linolenic acid and lignoceric acid). The dominant monounsaturated fatty acid of the oil is oleic acid, which accounted for 50.5% of the total fatty acid content, hence, the oil belongs to oleic acid category [28]. The oleic acid content of used soya oil is comparatively higher than 7-40% reported for coconut oil, palm oil and cottonseed oil [29], [30]. This shows that used soya oil is highly unsaturated triglycerides. Nevertheless, the fatty acid components of the used soya oil were found to be consistent with the fatty acids present in typical oils used for producing biodiesel.

3.3 Fourier Transform Infrared (FT-IR) Spectra Analysis of Used Soya Oil

The FTIR spectrum analysis of used soya oil was determined as shown in Figure 2. From the result, obvious peaks of note were recorded . The region 723.8 cm^{-1} ($679.61\text{ cm}^{-1} - 886.65\text{ cm}^{-1}$) indicate the presence of $=\text{C}-\text{H}$ (alkenes) functional groups. They possess bending type of vibrations appearing at low energy and frequency region in the spectrum and they are all double bounded. They are attributed to olefins (alkenes) functional groups and are unsaturated. The characteristics peak found in the region 1114.5 cm^{-1} ($1050.15 - 1297.23\text{ cm}^{-1}$) indicate stretching vibrations of C-O and C-O-C.They can also indicate the bending vibration of O-CH3 in the spectrum [31], [32]. The band region of 1375 cm^{-1} can be ascribed to the bending vibration of C-H methyl groups , while the band at 1401cm^{-1} ($1400-1800\text{ cm}^{-1}$) is ascribed to $\text{C}=\text{C}$ bending vibrations [33]. The peaks at 2855.75 cm^{-1} and 2922cm^{-1} indicate symmetric and asymmetric stretching vibrations of C-H alkane groups respectively. They could be methyl (CH3) or methylene groups

Empirical Modeling of Kinetics of Transesterification and Cold Flow Properties of Used Soya Oil Biodiesel

and they require high energy to cause stretching vibrations within their bond when compared to the ordinary C-H bending vibrations of alkene groups detected at low energy and frequency region [34], [35]. The peak at 3000cm⁻¹ is attributed

to the stretching vibration of =C-H alkene groups. They are detected above wave number 3000 cm⁻¹ in the spectrum compared to corresponding alkane C-H stretching groups detected below 3000 cm⁻¹

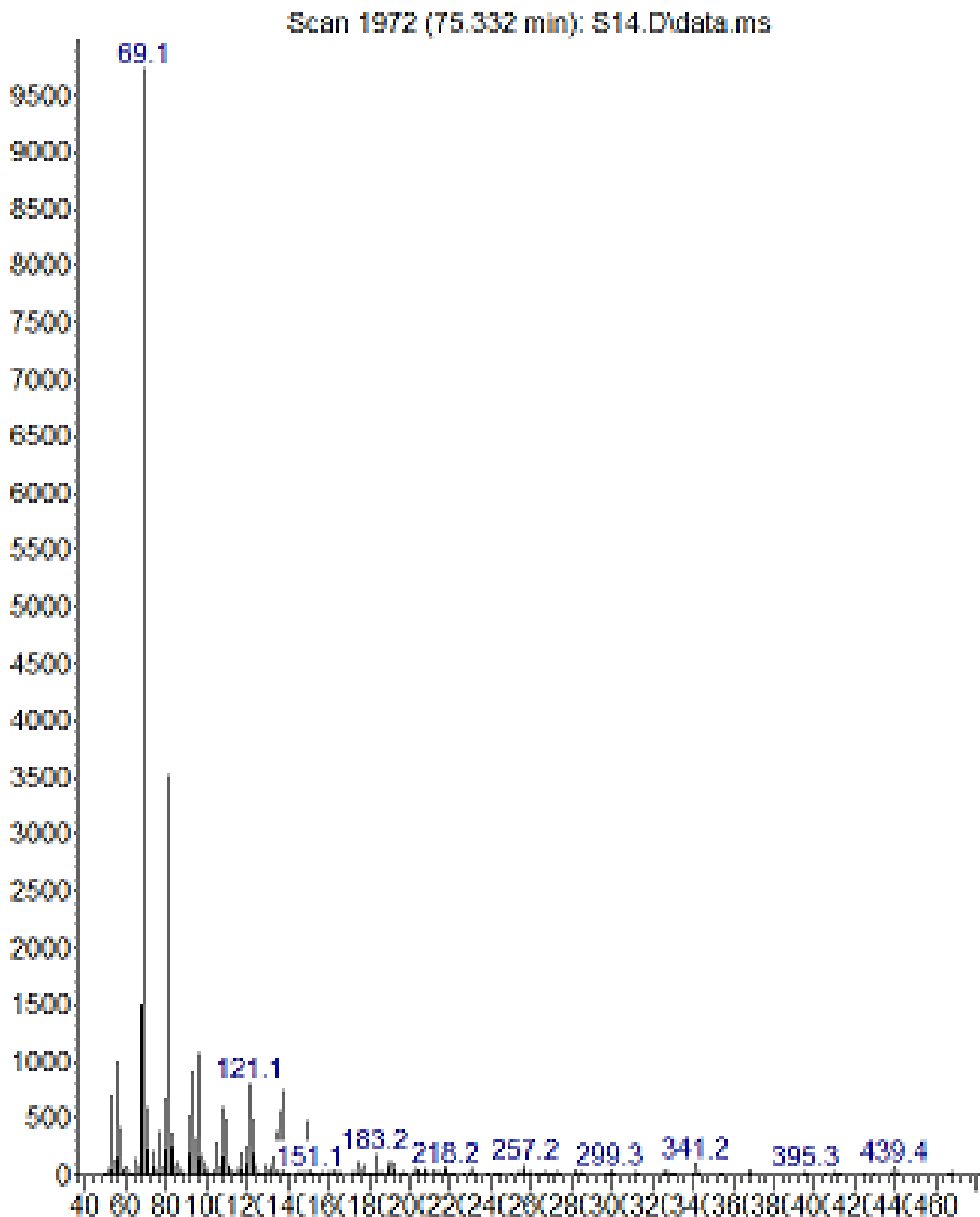


Figure 1: GC-MS Spectra of used soya oil

Table 2: Summary of fatty acid composition of used soya oil.

Fatty Acid	Structure	Composition (%)	Molecular weight (g/mol)
Myristic acid	C14:0	0.85	228.30
Oleic acid	C18:1	50.5	282.465
Stearic acid	C18:0	10.56	284.48
Palmitic acid	C16:0	20.56	256.4
Arachidic acid	C20:0	0.67	304.470
linoleic acid	C18:2	1.80	294.48
linolenic acid	C18:3	1.05	278.43
Lignoceric acid	C24:1	0.22	368.63

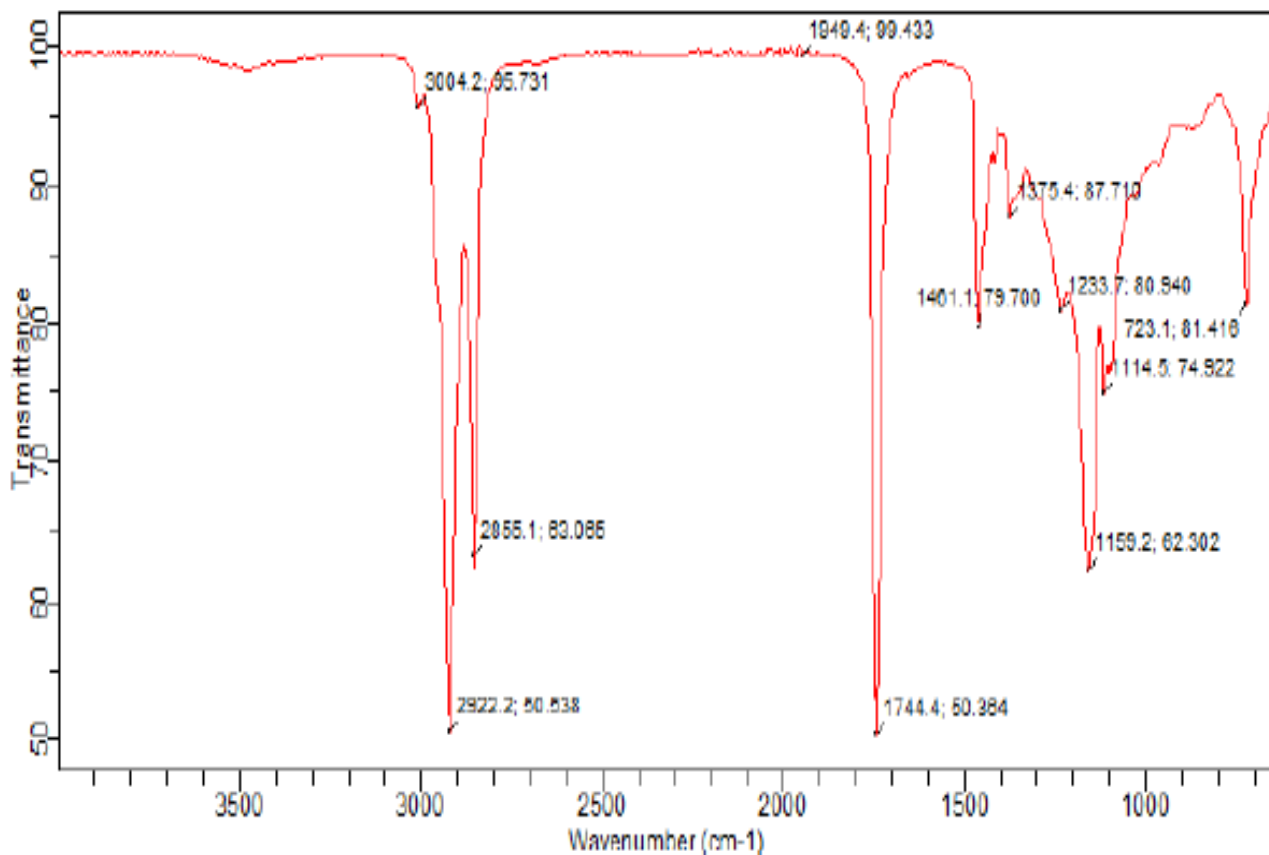


Figure 2: FT-IR spectra of used soya oil.

3.4 Fuel Properties of the FAME Produced

The summary of the fuel properties studied in the course of this research work is as given in table 3. The density and kinematic viscosity of the USOFAME, 863kg/m³ and 4.60mm²/s which are within the ASTM limits are higher than those of the USO, 962kg/m³ and 47.78mm²/s. High viscosity of the fuel results in poor atomization, incomplete combustion which leads to coking of injector tips and engine power loss. Low-viscosity fuel produces a very subtle spray which cannot get into the combustion cylinder, thus forming the fuel rich zone which lead to the formation of soot [36], [37]. From the result it could be

inferred that FAME from used soya oil have a good injection and atomization performance. Furthermore it will offer superior lubrication and protection for the moving parts of engine than the diesel. The flash point is a shows the degree of flammability of materials. The typical flash point of pure methyl ester is $\geq 1300\text{C}$, classifying them as “non-flammable”. However, during production and purification of biodiesel, not all the methanol may be removed, making the fuel flammable and dangerous to handle and store if the flash point falls below 1300C. The flash point is 1620C for used soya oil fatty acid methyl ester.. This is within the ASTM standard as shown in Table 3, indicative of the

Empirical Modeling of Kinetics of Transesterification and Cold Flow Properties of Used Soya Oil Biodiesel

safety of USOFAME in handling and storage. Cetane number serves as a measure of ignition quality of the fuel. This is the most pronounced change from vegetable oil to the transesterified product. Fuels with low cetane number show an increase in emission due to incomplete combustion. The lower limit for cetane number by ASTM standards is 51. The values obtained for used soya oil biodiesel is 61.00. Thus the obtained result which are within the acceptable ASTM limits indicates that the produced biodiesel possess good ignition response. The cloud point which is the lowest temperature of first appearance of wax-like material on cooling the biodiesel was determined as 00C, and the pour point which is the lowest temperature at

which the fuel will still pour was determined as -40C for used soya oil biodiesel. The cold filter plugging point is the lowest temperature at which the filter is plugged such that the fuel will no longer pass through the filter was determined as -2.80C in this work. The characteristics of the biodiesel produced is within the ASTM standards for biodiesel, as shown in Table 3. However the cloud and pour points might give rise to cold flow problems in cold season. This problem however could be overcome by the addition of suitable cloud and pour point depressants or by blending with diesel oil [38].

Table 3: Fuel properties of USOFAME

Properties	Unit	USOFAME	ASTM Standards	Test Method
Acid value	mgKOH/g	0.400	0.50	D664
Density	Kg/m ³	863	860-900	D93
Kinematic viscosity@ 400C	mm ² /s	4.60	1.9-6.0	D445
Water & sediment	%	0.5	0.5	D2209
Flash point	0C	162	100-170	D93
Cloud point	0C	0		D2500
Cetane number		61.00	48-65	D613
Refractive index		1.4710	1.38	
Specific gravity	Kg/m ³	0.873	0.860-0.900	
Calorific value	MJ/Kg	40.28	42.06	D35
Pour point	0C	-4		D97
Iodine value	gI ₂ /100g	30.60	42.46	D4067
Cold filter plugging point	0C	-2.8		D6371

3.5 Kinetics of transesterification of USO

Methanolysis of used soya oil using sodium hydroxide (NaOH) catalyst was carried out in batches at temperatures of 450C, 550C and 650C. The rate constants evaluated by solving the ODE 6 to 25 using polymath 5.1 software are as shown in table 4. From the table, it could be observed that the values of the forward rate constants, k₁, k₃, and k₅ for transesterification of USO are greater than those of the reverse reaction k₂, k₄ and k₆. This shows that the forward reaction greatly exceeded the reverse reaction which could be neglected for the operating experimental conditions. This conforms with the findings of [39], [40], who separately reported predominance of forward reaction compared with backward reaction in their report of transesterification of jatropha oil and waste sunflower oil respectively. The rate constant for conversion of triglyceride to diglyceride, k₁ was the lowest of all the forward reaction at all reaction temperature and this step could be considered the rate

limiting step (RLS). Again the rate constant for the RLS increased with increase in temperature. This shows that the rate limiting step for transesterification of USO is favored at high temperature, indicative of the fact that heat is required for the reaction. The plots of lnk versus 1/T of the Arrhenius equation 27 for evaluating the activation energy are given in figures 3 to 8. The activation energies obtained from evaluation of the slopes of the plots are as given in table 4. The activation energy of the RLS for palm oil transesterification has been reported by [41], and [42] to be in the range of 27.3 to 61.5 KJ/mol. The activation energy of the RLS for transesterification of USO in this work is 19.31KJ/mol. The two factors that affect the kinetics of transesterification of oil are the degree of saturation of the oil, affecting TG to DG reaction step and chain length distribution of the oil affecting MG to GL reaction step. As the degree of saturation of the soya oil is low therefore the activation energy is relatively low, showing ease of its transesterification.

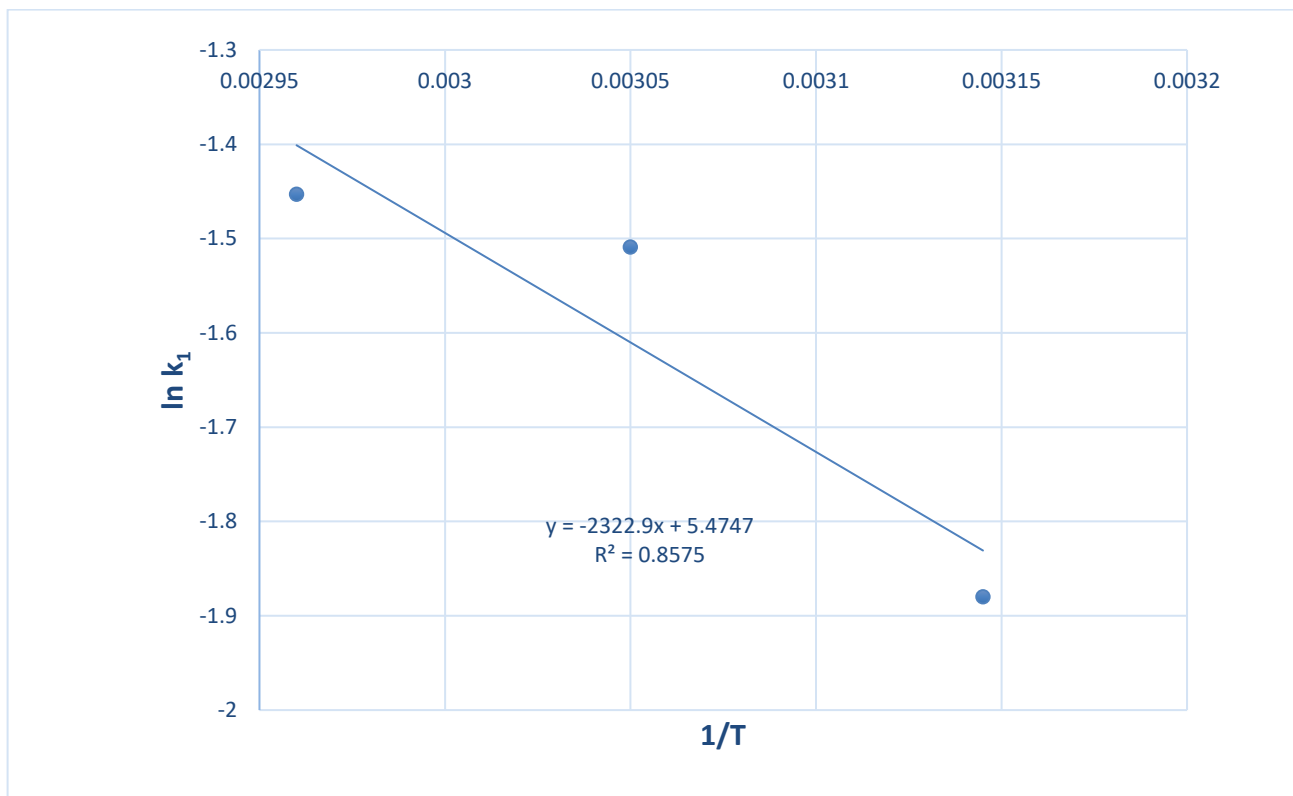


Figure 3: A plot of $\ln k_1$ VS $1/T$ for USOFAME

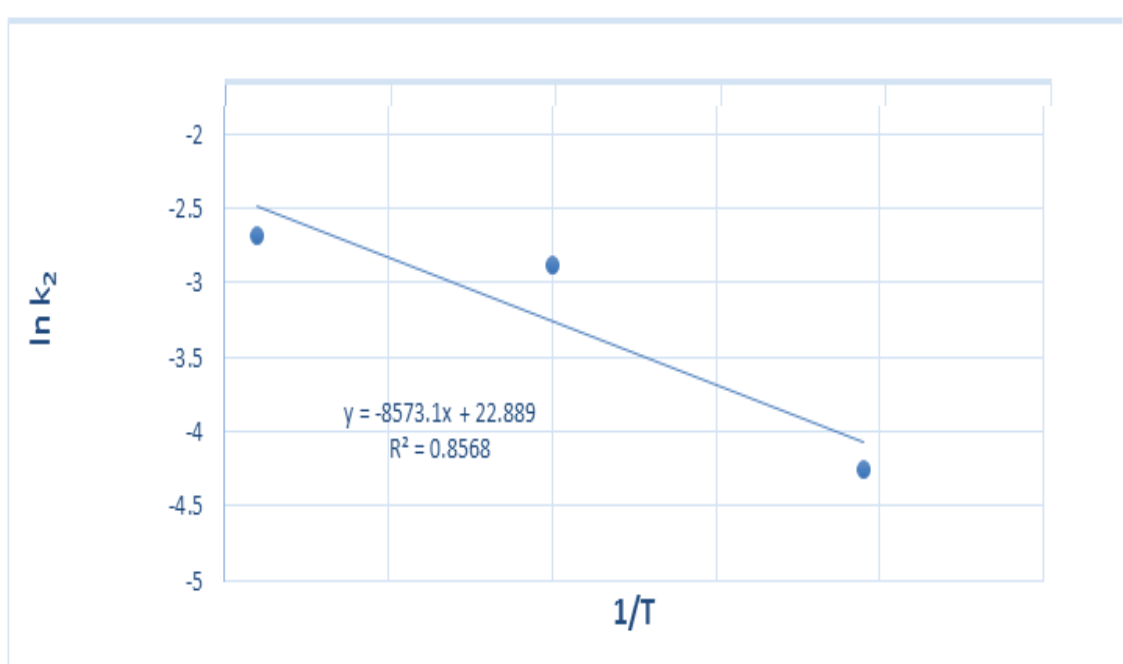


Figure 4: A plot of $\ln k_2$ VS $1/T$ for USOFAME

Empirical Modeling of Kinetics of Transesterification and Cold Flow Properties of Used Soya Oil Biodiesel

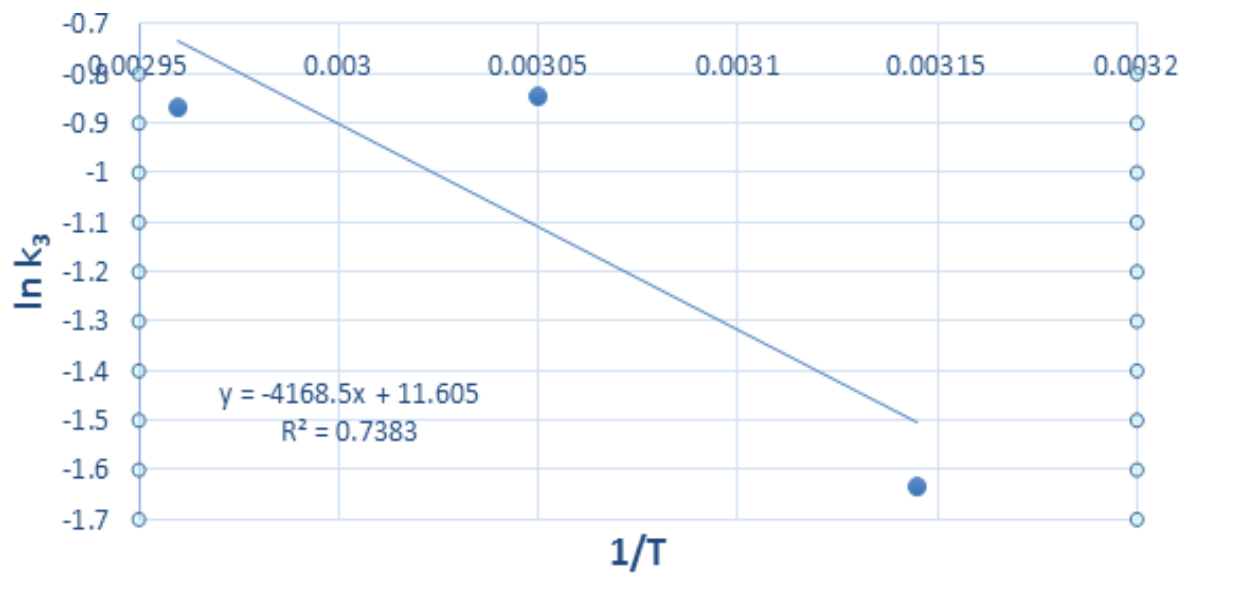


Figure 5: A plot of $\ln k_3$ VS $1/T$ for USOFAME

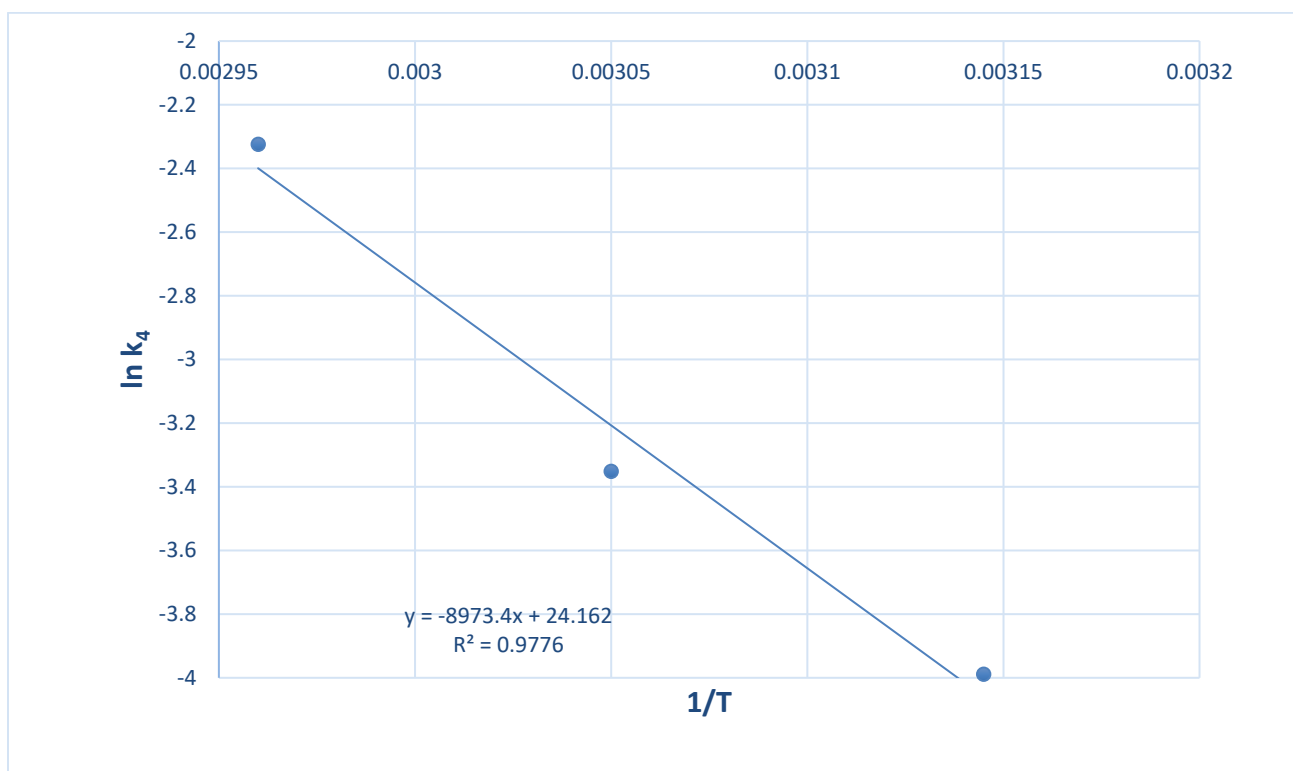


Figure 6: A plot of $\ln k_4$ VS $1/T$ for USofAME

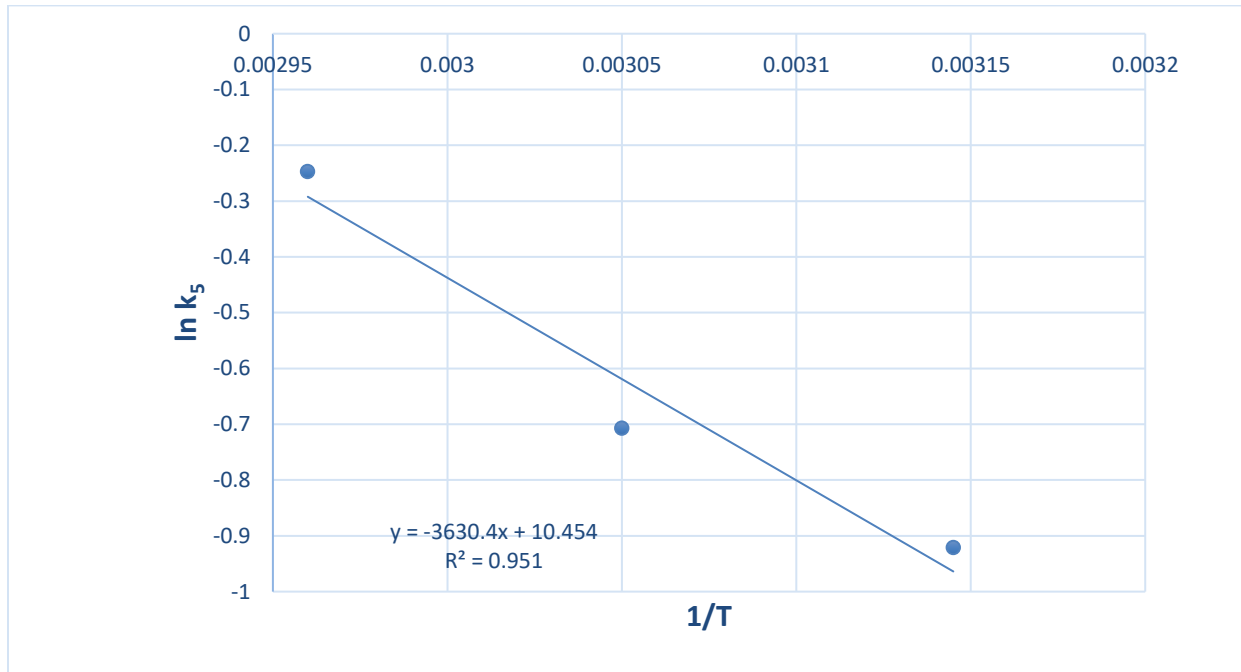


Figure 7: A plot of $\ln k_5$ VS $1/T$ for USOFAME

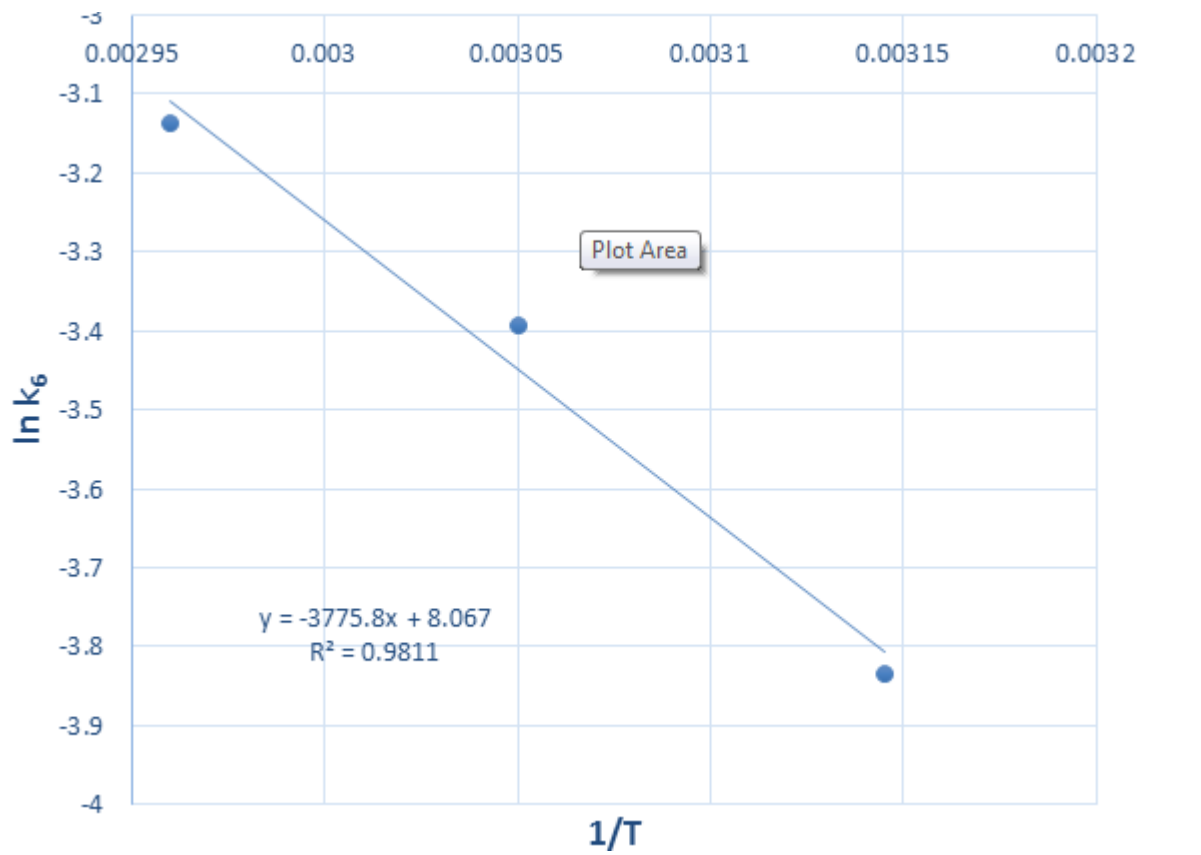


Figure 8: A plot of $\ln k_6$ VS $1/T$ for USOFAME

Empirical Modeling of Kinetics of Transesterification and Cold Flow Properties of Used Soya Oil Biodiesel

Table 4: Rate constants at different temperatures and activation energy for transesterification of used soya oil

Used soya oil transesterification	45oC	55oC	65oC	ΔE (kJ/mol)
k_1 (min ⁻¹)	0.165	0.223	0.234	19.31
k_2 (min ⁻¹)	0.0142	0.0559	0.0674	71.280
k_3 (min ⁻¹)	0.197	0.430	0.416	34.657
k_4 (min ⁻¹)	0.0189	0.035	0.0978	74.604
k_5 (min ⁻¹)	0.398	0.493	0.786	30.183
k_6 (min ⁻¹)	0.0216	0.0336	0.0437	31.392

Product distribution for used soya oil transesterification. The formation of products and disappearance of reactants at temperatures of 45, 55, 65oC for transesterification of used soya oil using NaOH catalyst are shown in Figures 9. The figures shows that the product concentrations (BD and GL)

increased with increases in reaction time while the reactants concentration (TG, DG, MG, and MN) decreased with increase in reaction time. The concentration of the intermediate reactants (DG and MG) however initially increased with increase in time and later decreased with increase in time. Overall, the change in

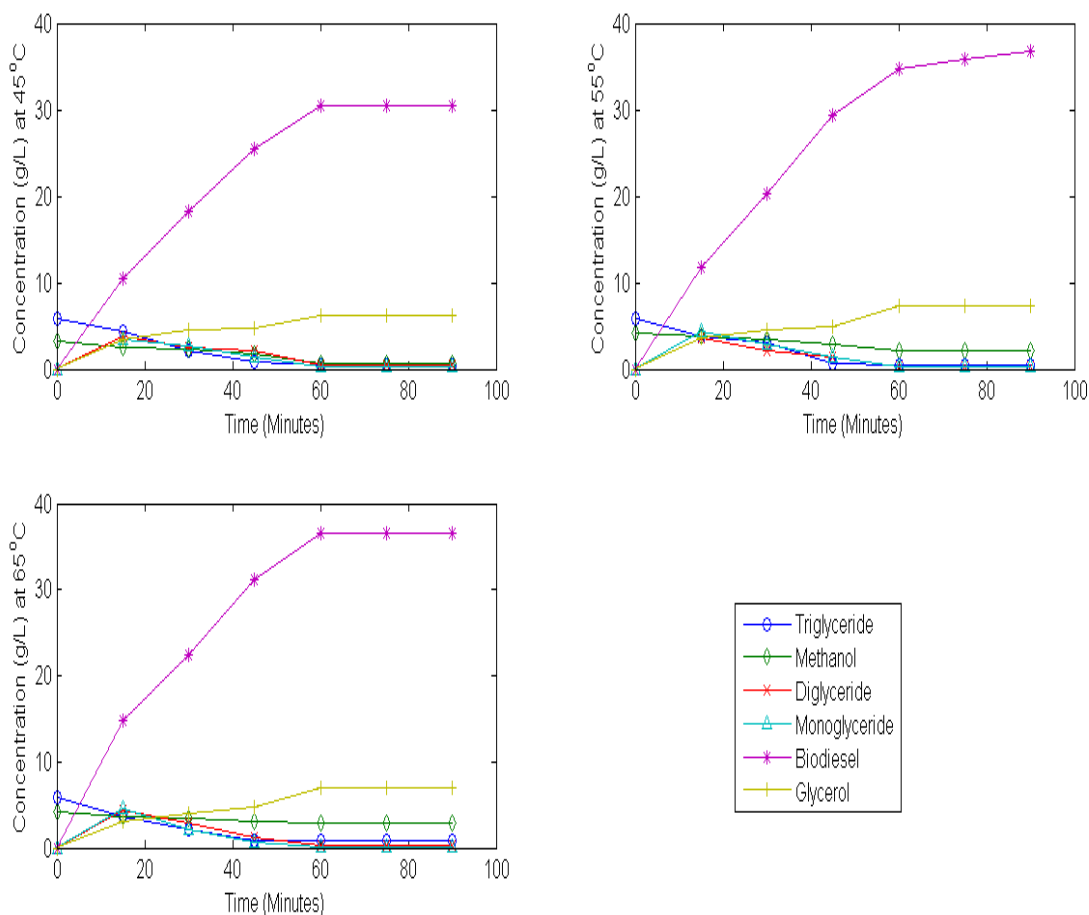


Figure 9: Product distribution for used soya oil transesterification at 45°C (a) at 55°C (b) at 65°C (c).

3.6 Modeling of effect of blending on cold flow properties of USOFAME

The cold flow properties of biodiesel are evaluated in terms of cold flow temperature operability, cloud point (CP), cold filter plugging point (CFPP), pour point (PP) etc. The values of the cold flow properties CP, CFPP and PP were determined experimentally for the various biodiesel fraction in the blends. The plot of variation of the cold flow temperature operability of the USOFAME mix with the biodiesel fraction is as given in figure 10. From the figure, it could be seen that the CP, CFPP and PP increased as the biodiesel fraction in the mix increased. The cloud point is of highest value while the pour point is the least. The modeling equations 2, 3,4 are fitted to data of figure 10 using least square regression of Microsoft excel. The correlation constants and the coefficient of determination of the models predicting cold flow temperature operability of the blend

as a function biodiesel fraction are as given in table 5. The correlation constants are used for calculation of the cold flow properties using the modeling equation while the coefficient of determination is used to discriminate between the fitting efficiency of the models to the data. The comparison between the measured and the predicted cold flow properties using modeling equations are given in table 6-8. The model with highest coefficient of determination is adjudged the best fitting model while the model with least percentage error difference between the measured and predicted values, gave credence to the degree of efficiency of data fitting by the model. From tables 5 and 7, it could be seen that the fitting model of highest coefficient of determination and least percentage error difference is polynomial model followed closely by the linear model. The polynomial model is therefore the best fitting model for predicting CP, CFPP and PP as a function of biodiesel fraction.

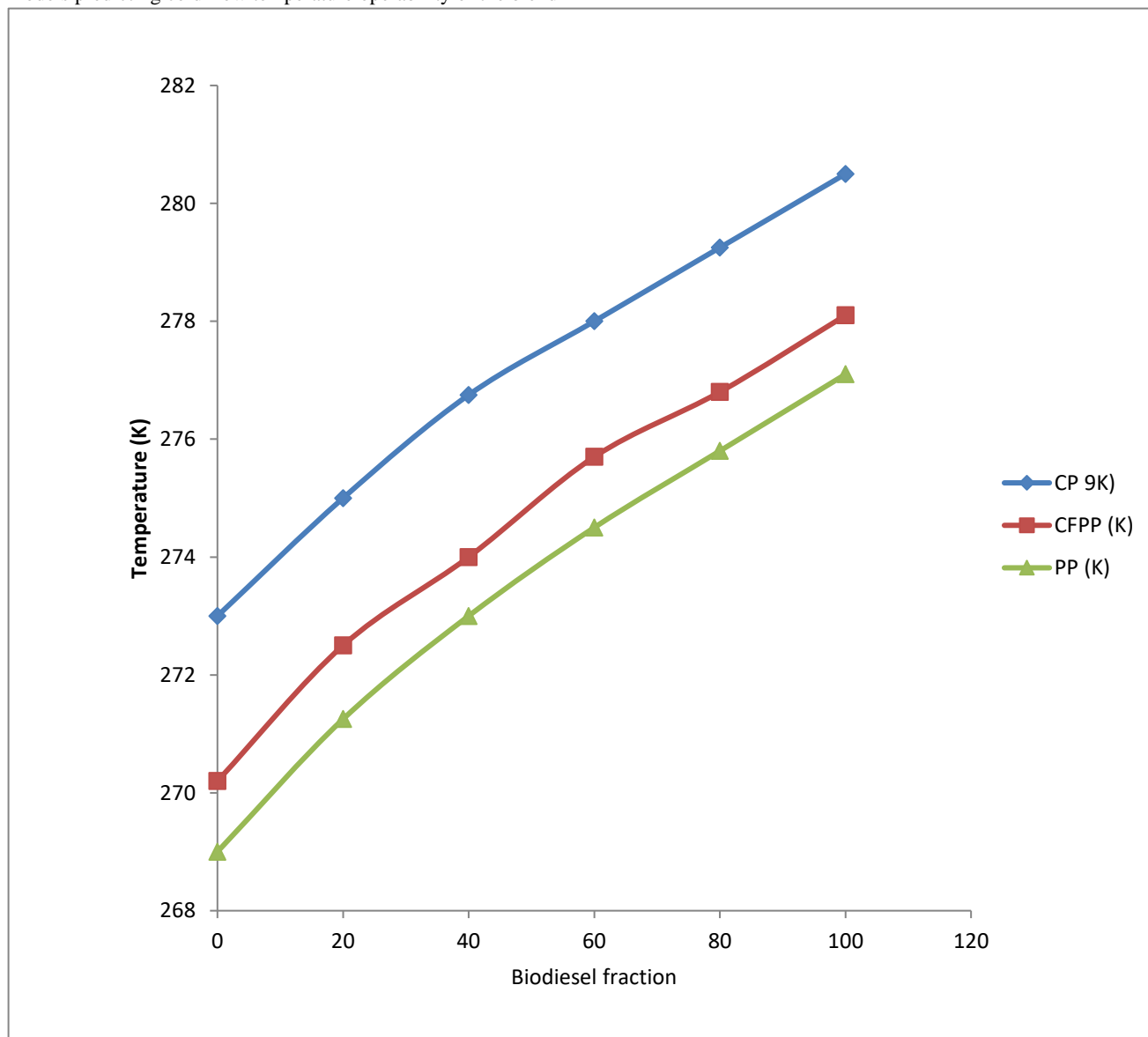


Figure 10: Effect of blending on cold flow properties of biodiesel

Empirical Modeling of Kinetics of Transesterification and Cold Flow Properties of Used Soya Oil Biodiesel

Table 5: Correlation constants and coefficient of determination of predicting models for CP, FPP and PP

Linear Model $Y = a + bx$											
CP				CFCP				PP			
a	B	R2		a	b	R2		a	B	R2	
273.5	0.072	0.984		270.5	0.078	0.981		269.4	0.079	0.987	
Exponential Model $Y = c + edx$											
CP				CFPP				PP			
c	D	R2		c	d	R2		c	d	R2	
273.5	0.000	0.983		270.5	0.000	0.980		269.4	0.000	0.986	
Polynomial Model $Y = f + g + hx^2$											
CP				CFPP				PP			
f	G	H	R2	f	g	H	R2	f	g	H	R2
273.1	0.099	0.000	0.996	270.2	0.106	0.000	0.998	260.9	0.108	0.000	0.999

Table 6: Comparison between measured and predicted CP, CFPP, and PP using linear model

BF	Meas. CP	Pred. CP	Perc. Deff.	Meas. CFPP	Pred. CFPP	Perc. Diff.	Meas. PP	Pred. PP	Perc. Diff.
0	273.00	273.00	0.00	270.20	270.15	-0.02	269.00	269.40	0.15
20	275.30	274.94	-0.13	272.50	272.06	-0.16	271.25	270.98	-0.10
40	276.15	275.88	-0.10	274.00	273.38	-0.23	273.00	272.56	-0.16
60	278.00	277.82	-0.19	275.70	274.82	0.32	274.50	274.14	-0.33
80	279.25	279.26	-0.01	276.81	276.74	-0.02	275.80	275.72	-0.03
100	280.50	280.70	0.07	278.10	277.70	0.15	277.10	277.30	0.07

Table 7: Comparison between measured and predicted CP, CPP and PP using exponential model

BF	Meas. CP	Pred. CP	Perc. Deff.	Meas. CFPP	Pred. CFPP	Perc. Diff.	Meas. PP	Pred. PP	Perc. Diff.
0	273.00	273.00	0.00	270.20	270.50	0.11	269.00	269.40	0.15
20	275.30	274.05	-0.45	272.50	271.04	-0.54	271.25	269.94	-0.48
40	276.75	274.60	-0.78	274.00	271.60	-0.88	273.00	270.48	-0.92
60	278.00	275.15	-1.03	275.70	272.13	-1.29	274.50	271.02	-1.26
80	279.25	275.70	-1.21	276.80	272.67	-1.49	276.80	271.56	-1.89
100	280.50	276.25	-1.52	278.10	275.22	-1.75	277.00	272.11	-1.76

Empirical Modeling of Kinetics of Transesterification and Cold Flow Properties of Used Soya Oil Biodiesel

Table 8; Comparison between measured and predicted CP,CFPP and PP using polynomial model

BF	Meas. CP	Pred. CP	Perc. Diff.	Meas. CFPP	Pred. CFPP	Perc. Diff.	Meas. PP	Pred. PP	Perc. Diff.
0	273.00	273.10	0.04	270.20	270.20	0.00	269.00	269.00	0.00
20	275.30	275.08	-0.08	272.50	272.32	-0.07	271.25	271.16	-0.03
40	276.75	277.06	-0.11	274.00	274.44	0.16	273.00	273.32	0.12
60	278.00	279.04	0.39	275.70	276.56	-0.31	274.50	275.48	0.36
80	279.25	280.02	0.28	276.80	278.68	0.68	275.80	277.64	0.66
100	280.50	283.00	0.89	278.10	280.08	0.71	277.10	279.98	1.04

Legends: BF = biodiesel fraction, Meas.=measured, Perc. Diff. =percentage difference, Pred. =predicted

4. CONCLUSION

Kinetic modeling of transesterification of USO provided data for detailed experimental design of transesterification of the oil such as activation energy at different temperatures, forward and reverse rate constants, k_1 , k_2 , k_3 , k_4 , k_5 , k_6 and revealed the RLS as the conversion of TG to DG. Modeling of cold flow properties with biodiesel fraction gave the values of cold flow temperature operability, CP, CFPP, and PP for given the biodiesel fractions in the blends. Polynomial model proved the best fitting model for cold flow properties as a function of biodiesel fraction.

REFERENCES

- Issariyakul, T., Kulkarni M.G., Meher, L.C., Dalai, K.K. and Bukahshi, N.N. (2008). Biodiesel production from mixture of canola and used cooking oil. *Chemical Engineering Journal* 140: 77-85.
- Fukuda, H., Kondo, A. & Noda, H. (2001). Biodiesel fuel production by transesterification of oils, *Bioscience Bioengineering Journal*, 92, 405-416.
- Lee, S and Shah, Y. T. (2013). *Biofuels and Bioenergy: Processes and Technologies*. CRC Press, Taylor and Francis Group,
- 600 Broken Sound Parkway NW, Suite 300 Boca Raton, FL. ISBN 978-1-4200-8955-4. Gerpen, V.J. (2005). *Biodiesel Processing and Production*. *Fuel Processing Technology*. J.86(10) 1097-1107.
- Gui, M., Lee, K. & Bhatia, S. (2008). Feasibility of edible oil vs. non-edible oil vs. waste edible oil as biodiesel feedstock. *Energy* 33(11): 1646-1653.
- NanthaGopal, K., Arindam, P., Sumit, S., CharanSamanchi, K. Sathyanarayanan, T. & Elango, A. (2014). Investigation of emission and combustion characteristics of a CI engine fueled with waste cooking oil methyl ester and diesel blends, *Engineering Journal*, 53, 281- 287.
- A. Demirbas, (2009). "Progress and recent trends in biodiesel fuels". *Energy Conversion and Management* 50, 14-34
- Leung, D.Y.C. & Guo, Y. (2010). Transesterification of meat and used frying oil: Optimization for biodiesel production. *Fuel Process Technology*, 87, 883-890.
- Lu, H., Liu, Y., Zhou, H., Yang, Y., Chen, M. & Liang, B. (2009). Production of biodiesel from *Jatropha curcas* L. oil. *Computer and Chemical Engineering* 33(5), 1091-1096.
- Aderemi, B.O. and Hamid, B.H. (2010). Production of Biodiesel from palm oil. *Nigerian Society of Chemical Engineers Proceedings*, 40, 135-143. Abuja Nigeria.
- Younis, M. N., Saeed, M. S., Khan, S., Furqan, M. U., Khan, R. U. & Saleem, M. (2009). Production and characterization of biodiesel, from waste and vegetable oils. *Journal of Quality and Technology Management*, 5(1), 111-121.
- Attanatho, L., Magmee, S., Jenvanitpanjakul, P. (2004). Factors affecting the synthesis of biodiesel from crude palm kernel oil. *The Joint International Conference on Sustainable Energy and Environment (SSE)*, Hua Hin, Thailand, 1-3 December 2004.
- Lopez, L., Bocanegra, J., Malagon-remero, D., (2015). Production of biodiesel from waste cooking oil by transesterification, *Ingenieria y Universidad*, 19(1), 155-172.
- Alarcon, R., Malagon-Romero, D., Ladino, A, 2017. Biodiesel production from waste frying oil, *Chemical Engineering Transaction*, 57, 571-576.
- Rodriguez, D., Riesco, J., Malagon-Romero, D., (2017). Production of biodiesel from waste cooking oil and castor oil blends. *Chemical Engineering Transaction*, 57, 679-684.
- Sarin, A., Arora, R., Singh, N.P., Sarin, R., Malhotra, R.K., Kundu, K., "Effect of blend of palm, jatropha, pongamia biodiesel on cloud point and pour point", *Energy* 2009, 34, pp2016-2021.
- Ezekannagha, C.B., Nwabueze, H.O., Ekeke, J.A. Empirical Models and Rheology of some Basic Properties of Lard Biodiesel and their Blends with Diesel fuel. *Journal of Emerging Trends in Engineering and Applied Sciences (JETEAS)* 7(3): 149-160, 2016.
- Ogunsuyi, H.O. (2015). Production of biodiesel using African pear (*Dacryodes edulis*) seed oil as feedstock. *Academic Journal Biotechnology* 3(5), 085-092.
- Hanumanth, M., Hebbal, O.D. & Navindgi, M.C. (2012). Extraction of biodiesel from vegetable oil and their

- comparisons; *International Journal of Advanced Scientific Research and Technology*, 2(2), 2249-9954.
20. Akpan, U.G., Jimoh A. and Mohammed, A.D. (2006) Extraction, Characterization and Modification of Castor Seed Oil. *Leonardo Journal of Science*.
 21. Freedman, B., Pryde, E.H. & Mounts, T.L. (1999). Variables affecting the yields of fatty esters from transesterified vegetable oils, 61, 1638–1643.
 22. Berchmans, H.J., & Hirata, S. (2008). Biodiesel Production from Crude *Jatropha Curcas L.* Seed Oil with a High Content of Free Fatty Acids. *Bioresour Technol*, 99, 1716-1721.
 23. Umezuegbu J.C., Ezennajiego E. E., Onukwuli O. D. Production, Characterization and Optimization of Biodiesel from *Gmelina* seed oil. *World Journal of Innovative Research (WJIR)*, 8(4) April 2020 pp74-86.
 24. Lapuerta, M., Armas O. & Fernandez, J.R. (2008). Effect of Biodiesel Fuels on diesel engine emissions. *Progress in Energy and Combustion Science*, 34, 198-223
 25. Demirbas, A. (2003) Biodiesel Fuel from vegetable oils via catalysis and non-catalysis supercritical alcohol transesterification and other methods. *Energy Conversion Manag.* 44,2093-2109.
 26. Mustapha, O.A., Adebisi, A.A., and Olanipekun, B.O. Characterization of biodiesel from alkaline refinement of waste cooking oil. *International Annals of Science*, 10(2), pp16-24(2021).
 27. Zahoor, U., Mohamad, A.B., and Zakaria, M. Characterization of waste palm cooking oil for biodiesel production. *International Journal of Chemical Engineering and Applications*, 5(2), April 2014.
 28. Sonntag, A. (2012). Reaction of fats and fatty acids. In: Balley (Eds) *Industrial Oil and Fat Products*, fourth ed. Wiley, New York USA, 99-120.
 29. Ampaitepin, S., Miyuki, K. & Tetsuo, T. (2006). Life cycle analysis of biodiesel fuel production: Case study of using used cooking oil as a raw material. Kyoto, Japan. Proceeding 2nd Joint International Conference on Sustainable Energy and Environment, SEE, 21-23. November 2006, Bangkok, Thailand.
 30. Rashid, U. and Anwar, F. (2008). Production of Biodiesel through Optimized Alkaline Catalyzed Transesterification of Rapeseed Oil. *Fuel*, 87, 265 – 273.
 31. John, C. (2000). Interpretation of infrared spectra, a practical approach. *Encyclopedia of analytical chemistry*, R.A. Meyers (Ed). John Wiley and Sons Ltd, Chichester, 10815-10837.
 32. Isah, Y., Yousif, A.A., Feroz, K.K., Suzana, Y., Ibraheem, A. & Soh C. (2015) Comprehensive characterization of napier, grass as feedstock for thermochemical conversion. *Open Access Energies Journal*, 8:3403-3417.
 33. Shuit, S.H., Lee, K.T., Kamaruddin, A.H. & Yusup, S. (2010). Reactive extraction and in situ esterification of *Jatropha curcas L.* seed for production of biodiesel. *Fuel*, 89, 520-527.
 34. Saifuddin, N. & Refai, H. (2014). Spectroscopy analysis of structural transesterification in biodiesel degradation. *Research Journal of Applied Sciences, Engineering and Technology*, 8(9), 1149–1159.
 35. Jimoh, A., Abdulkareem, A.S., Afolabi, J.O. & Odigure Odili U.C. (2012). Production and characterization of biofuel from refined groundnut oil. 10–12.
 36. Endah, M.M.P., Rachimoallah, M., Nidya, S. & Ferdy, P. (2012). Biodiesel production from kapok seed oil (*Ceiba pentandra*) through the transesterification process by using Cao as catalyst, *International Research Journal*, 12(2), 3-7.
 37. Ezekwe, C. C. & Ajiwe, V. (2014). The variations of physiochemical properties of biodiesel blends with the blend ratios. *International Journal of Science Innovations and Discoveries*, 4 11 -14.
 38. Prafulla, D. P., Veera, G. G., Harvind, K. R., Tapaswy, M. & Shuguang, D. (2012). Biodiesel production from waste cooking oil using sulfuric acid and microwave irradiation processes. *Journal of Environmental Protection*, 3, 111-117.
 39. Muazu, K., Mohammed-Dabo I, I.A., Waziri, S.M., Ahmed, A.S., Bugaje, I.M., Zanna, U.A.S. Kinetic modeling of transesterification of *Jatropha curcas* seed oil using heterogeneous catalyst, *Eng Technol* 2(3) :87-94 (2015).
 40. Klofutar, B., Golob, J., Licozar, B., Klofutar, C., Zagar, E. Transesterification of rapeseed and waste sunflower oils: Mass transfer and kinetics in a laboratory batch reactor and in an industrial -scale reactor/separator setup. *Bioresour Technol* 101:3333-3344 (2020).
 41. Danako, D., and Cheryan, M. Kinetics of palm oil transesterification in a batch reactor. *Journal of the American Oil Chemists' Society* 77(12): 1263-1267 (2000).
 42. Su, Y., Wang, H., and Bao, G. Transesterification kinetics of biodiesel production from palm oil. *Huaxue Gongcheng* 38(11): 39-42 (2020).